

## Supporting Information

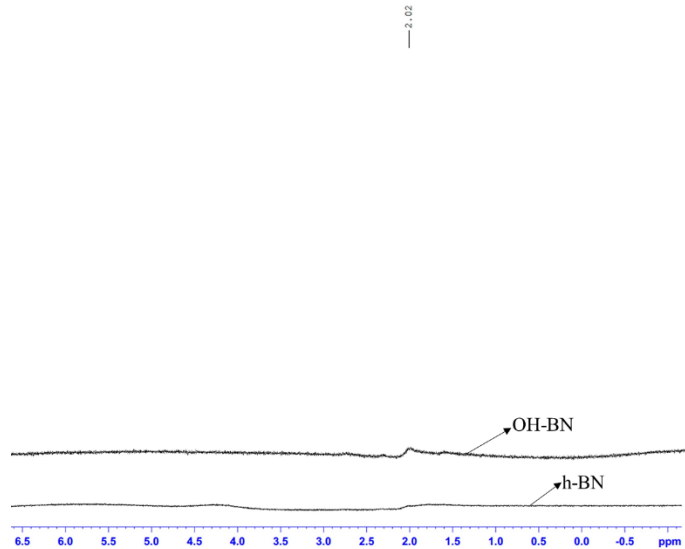
### High-Yield Synthesis of Hydroxylated Boron Nitride Nanosheets and Their Utilization in Thermally Conductive Polymeric Nanocomposites

*Feng Yuan<sup>a&</sup>, Qinhan Guan<sup>a&</sup>, Xuehan Dou<sup>a</sup>, Han Yang<sup>a</sup>, Yiming Hong<sup>a</sup>, Yawen Xue<sup>a</sup>, Zhenxing Cao<sup>a</sup>, Haiyan Li<sup>b</sup>, Zexiao Xu<sup>c</sup>, Yuyang Qin<sup>\*a, b, c</sup>*

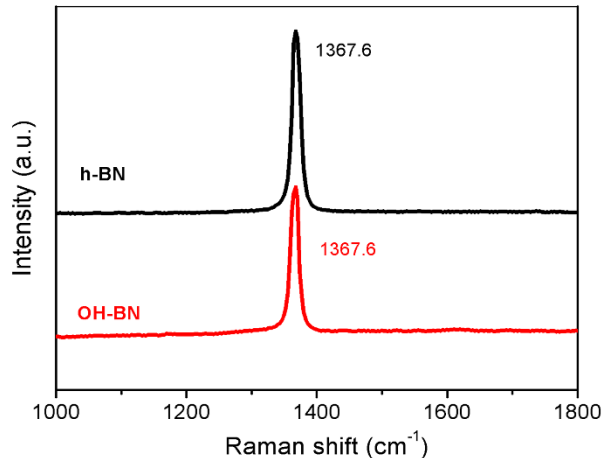
<sup>a</sup> *School of Materials Engineering, Changshu Institute of Technology, Changshu, 215500, China.*

<sup>b</sup> *College of Chemistry and Chemical Engineering, Northeast Petroleum University, Daqing, 163318, China*

<sup>c</sup> *Suzhou Jiren High-Tech Materials Co., Ltd, Suzhou, China*



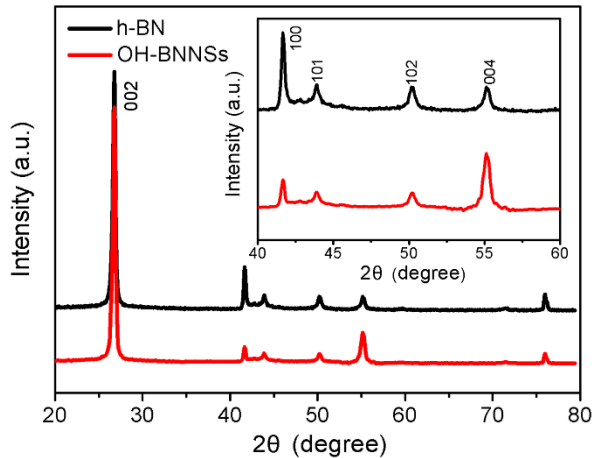
**Fig. S1** solid-state  $^1\text{H}$  NMR of h-BN and OH-BN.



**Fig. S2** Raman spectra of the pristine h-BN powders and the as-produced OH-BN

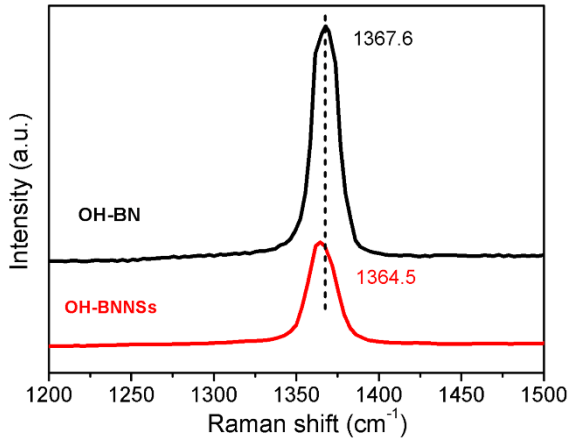
Clearly, the Raman spectrum of the OH-BN shows no new features in comparison with that of the raw h-BN. The high frequency  $E_{2g}$  mode of OH-BN appears at  $1367.6\text{ cm}^{-1}$ , which is identical to that of the pristine h-BN, indicating that the hexagonal structure of h-BN is well preserved after oxidation<sup>1</sup>.

## Preparation of OH-BNNSSs by the decomposition of H<sub>2</sub>O<sub>2</sub>



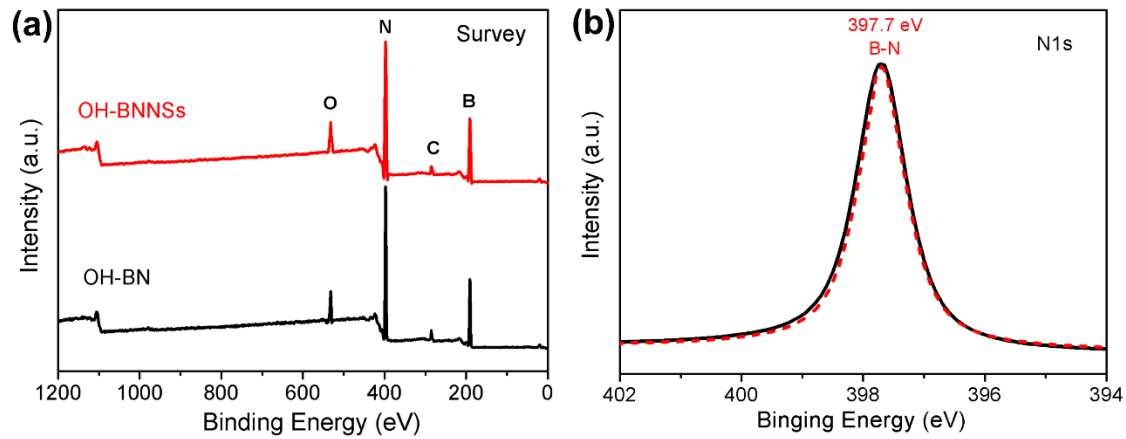
**Fig. S3** XRD patterns of the raw h-BN and the as-synthesized OH-BNNSSs

Fig. S3 shows the comparative XRD curves of the h-BN and OH-BNNSSs, it is observed that the initial h-BN powders exhibit a well crystallized structure, showing a series of distinct diffraction peaks, corresponding to the (002), (100), (101), (102) and (004) planes (JCPDS Card 34-0421), respectively. The XRD pattern of OH-BNNSSs matches well with that of the raw h-BN, suggesting that there is no damage to the hexagonal lattices of h-BN during exfoliation.<sup>2</sup> From the amplified patterns in its inset, we can see that the intensity of (004) peaks of OH-BNNSSs is unusually intensive, by taking the intensity of the (100) plane as a reference. As we all know, the exfoliation process will occur on the (002) plane, thus resulting in more (002) planes. When OH-BNNSSs are dispersed randomly in a glass sheet, they tend to lie on their widest facets. Certainly, the widest facets are the preferential orientations, i.e., the (002) (or 004) planes during the XRD detection. Therefore, the XRD result further confirms the occurrence of a very efficient exfoliation.<sup>3</sup>



**Fig. S4** Raman spectra of the OH-BN and OH-BNNs.

As the sensitivity of Raman signals to analysis the interlayer effects has been confirmed by previous report,<sup>4,5</sup> the Raman technique was employed to track the exfoliation effects of our method. Owing to a significant reduction in thickness, Raman active  $E_{2g}$  mode will show a red-shift or blue-shifting.<sup>6</sup> Bi-layered or few-layered nanosheets can be identified by a red shift, which is ascribed to a softening of the phonons caused by the slightly elongated B-N bonds. Whereas, a blue-shift of  $2\text{-}4\text{ cm}^{-1}$  will occur upon exfoliation to monolayer BN. This behavior is explained by the slightly shorter B-N bonds in monolayer, which result in a hardening of the phonons. As shown in Fig.S4, initially for the bulk OH-BN, the  $E_{2g}$  phonon mode is centered at  $1367.6\text{ cm}^{-1}$ . The OH-BNNs, however, exhibit the  $E_{2g}$  phonon mode at  $1364.5\text{ cm}^{-1}$ , corresponding to a red shift of  $\sim 3\text{cm}^{-1}$ . This support the assertion that few-layer OH-BNNs are peeled off from their host materials.



**Fig. S5** (a) The XPS survey scans of the OH-BNNSSs and OH-BN show that the OH-BNNSSs exhibit essentially the same compositions as the OH-BN. (b) High-resolution B1s XPS scans of the OH-BNNSSs shows that N atoms are bound only to B atoms, without any oxygen.

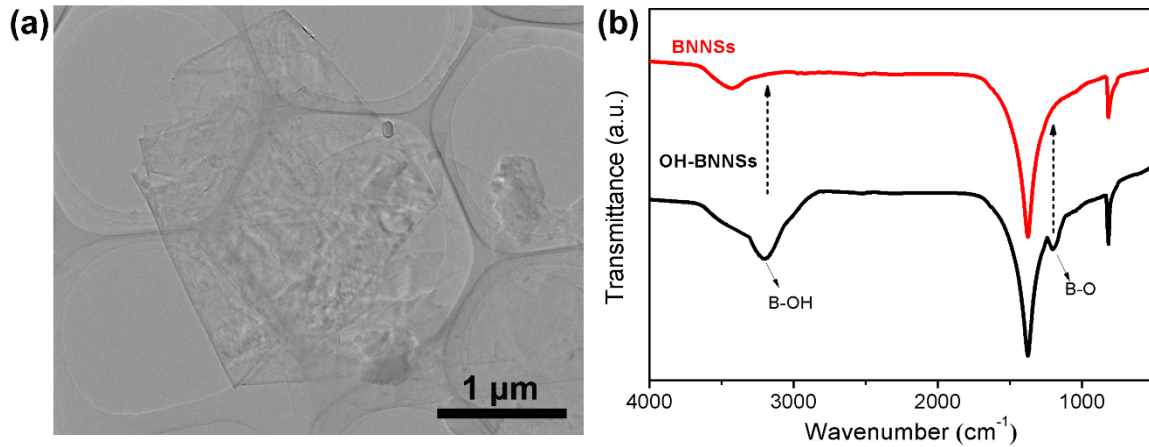


**Fig. S6(a)** The TEM image of the BNNSSs obtained by direct treatment of h-BN powders in  $\text{H}_2\text{O}_2$  under alkaline solutions. Ultrathin nanosheets were successfully prepared. **(b)** The FT-IR spectra of BNNSSs and OH-BNNSSs show that the lack of-OH groups on the BNNSSs surfaces, as the two peaks assigned to B-O-H vibrations both disappear in BNNSSs.



**Fig. S7** Digital photograph images of BNNsS and OH-BNNsS suspensions in ethanol, IPA and DMF for 1 week after sonication. The inset shows digital photograph images of these three dispersions from a week ago.

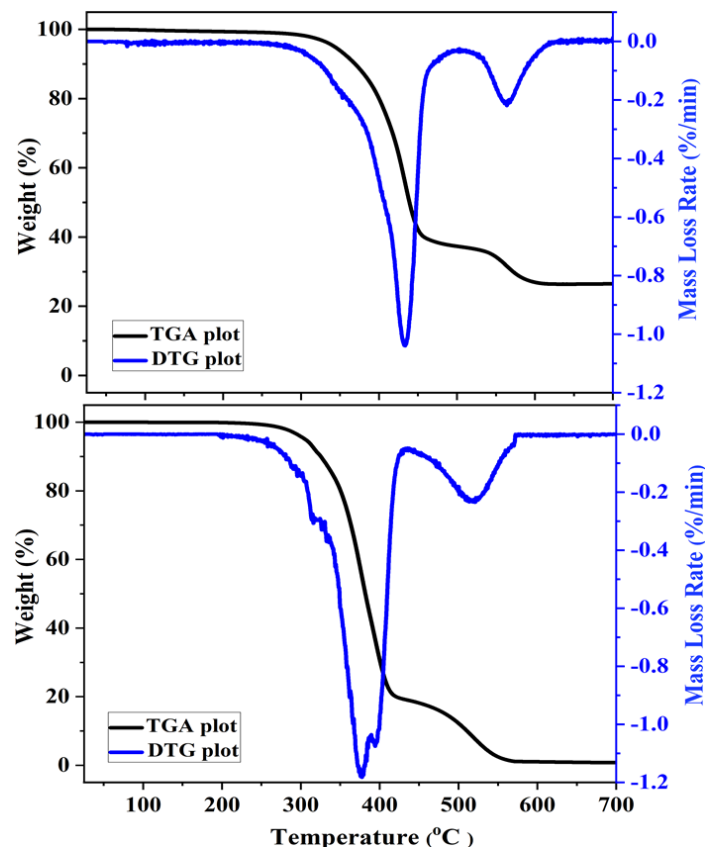


**Fig. S8** TGA-DTG plots of the pure TPU resin (down) and the TPU composite containing 30wt% OH-BNNSs (up)

## Reference

1. R. J. Nemanich, S. A. Solin and R. M. Martin, *Physical Review B*, 1981, 23, 6348-6356.
2. D. Lee, B. Lee, K. H. Park, H. J. Ryu, S. Jeon and S. H. Hong, *Nano Letters*, 2015, 15, 1238-1244.
3. Y. Xue, Q. Liu, G. He, K. Xu, L. Jiang, X. Hu and J. Hu, *Nanoscale Research Letters*, 2013, 8, 49.
4. L. Song, L. Ci, H. Lu, P. B. Sorokin, C. Jin, J. Ni, A. G. Kvashnin, D. G. Kvashnin, J. Lou, B. I. Yakobson and P. M. Ajayan, *Nano Letters*, 2010, 10, 3209-3215.
5. R. V. Gorbachev, I. Riaz, R. R. Nair, R. Jalil, L. Britnell, B. D. Belle, E. W. Hill, K. S. Novoselov, K. Watanabe, T. Taniguchi, A. K. Geim and P. Blake, *Small*, 2011, 7, 465-468.
6. G. R. Bhimanapati, D. Kozuch and J. A. Robinson, *Nanoscale*, 2014, 6, 11671-11675.